RSC Advances

PAPER

View Article Online
View Journal | View Issue

Cite this: *RSC Adv.*, 2021, **11**, 19902

Re(I)-nitroxide complexes†

Kseniya Maryunina, *[a] Gleb Letyagin, [ab] Artem Bogomyakov, [abc] Vitaly Morozov, [ab] Sergey Tumanov, [ab] Sergey Veber, [ab] Matvey Fedin, [ab] Evgeniya Saverina, [c] Mikhail Syroeshkin, [c] Mikhail Egorov, [c] Galina Romanenko [a] and Victor Ovcharenko [ac]

Received 18th March 2021
Accepted 25th May 2021

DOI: 10.1039/d1ra02159a

rsc.li/rsc-advances

Spin-labeled cyrhetrenes [(NNCp)Re(CO)$_3$] and [(INCp)Re(CO)$_3$], where NNCp is nitronyl nitroxide 2-(η^5-cyclopentadienyl)-4,4,5,5-tetramethyl-4,5-dihydro-1*H*-imidazole-3-oxide-1-oxyl and INCp is the corresponding imino nitroxide, were synthesized and characterized by EPR, CV, XRD, magnetochemistry and quantum chemistry methods. The correlations between different arrangements of paramagnetic centers and the magnetic exchange interactions for three polymorphs of [(NNCp)Re(CO)$_3$] were studied. It was concluded that high kinetic stability of nitroxide-substituted cyrhetrenes is a promising feature of compounds for the creation of multifunctional contrast agents.

Introduction

In recent years, the design of cyrhetrene derivatives [(RCp)Re(CO)$_3$] exhibiting pharmacological activity has been of significant interest.[1–3] The robust coordination of the η^5-cyclopentadienyl ligand and the low-spin d^6 electronic configuration of Re(I) provide high kinetic stability of this class of compounds under ambient conditions.[1–4] This makes cyrhetrenes suitable prototypes for developing the synthesis of their technetium and manganese analogs, which are much less radio-, photo-, and electrochemically stable.[1–5]

The possibility of introducing various functional substituents into the cyclopentadienyl ring, small size and the ability to mimic the benzene ring of the [(Cp)Re(CO)$_3$] fragment open the broad prospects for the creation of theranostics drugs providing both a targeted therapy and monitoring their accumulation and removal *in vivo*.[1,3,4] Despite the high potential of cyrhetrens for use in chemotherapy, photodynamic therapy, and radiological treatment by $^{186/188}$Re isotopes, only single-photon emission computed tomography based on ^{99m}Tc agents has become widespread for the noninvasive diagnostic localization of pathological processes.[1,3,4] Alternative methods for visualization of carbonyl complexes Re(I)/Tc(I) in tissues and organs based on fluorescence or UV/FTIR/Raman microscopy have a number of limitations[3,4] and require the use of complex facility, often equipped with specific sources of laser or synchrotron radiation.[3]

Another promising approach to the creation of rhenium(I) compounds for theranostics in our view is the combination in one molecule of cyrhetrene moiety and paramagnetic organic fragments for their use as contrast agents in magnetic resonance imaging. Kinetic stability, low toxicity and effective contrast properties of 2-imidazoline nitroxide radicals[6–9] are promising for their introduction as spin-labeled substituents R in [(RCp)Re(CO)$_3$] derivatives. However, the synthesis and physicochemical properties of such compounds are a scarce studied area of organometallic chemistry. Previously, a ferrocene and ruthenocene/osmocene species substituted with various nitroxide fragments have been extensively explored, while other nitroxide-bound derivatives of metallocenes,[10–15] including half-sandwich ones, are still unknown. We succeeded in synthesizing organometallic complexes [(RCp)Re(CO)$_3$] bearing nitroxide substituents R that could be used as a convenient approach in the design of paramagnetic targeted drugs for theranostics.

Results and discussion

Cyrhetren derivatives substituted with 2-imidazoline nitroxides were synthesized by the Ullman's method.[16,17] The nitronyl nitroxide [(NNCp)Re(CO)$_3$], imino nitroxide [(INCp)Re(CO)$_3$] and their diamagnetic precursor [(BHACp)Re(CO)$_3$] (Scheme 1) are kinetically stable both in the solid state and in solutions, and do not require special precautions when handling them. It could be suggested that an electrochemical impact or other physical stimuli are capable to induce electron transfer between

[a]*International Tomography Center SB RAS, Institutskaya Str. 3a, 630090 Novosibirsk, Russia. E-mail: mks@tomo.nsc.ru*

[b]*Novosibirsk State University, Pirogova Str. 1, 630090 Novosibirsk, Russia*

[c]*N. D. Zelinsky Institute of Organic Chemistry RAS, Leninsky Prospect, 47, Moscow, 119991, Russia*

† Electronic supplementary information (ESI) available: Experimental details relating to the synthesis, EPR spectroscopy and electrochemical studies, single crystals XRD experiments and crystallographic data, magnetochemistry measurements, fitting and analysis, and procedures and results of quantum-chemical calculations. CCDC 2064831–2064835. For ESI and crystallographic data in CIF or other electronic format see DOI: 10.1039/d1ra02159a

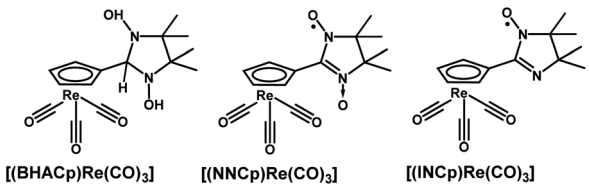

Scheme 1

the nitroxide fragment and the Re^{1+} ion.[18,19] However, as the results of electrochemical measurements, magnetochemical studies and quantum chemical calculations show below, intramolecular redox processes are not inherent of this type of compounds.

EPR spectroscopy study of [(NNCp)Re(CO)$_3$] and [(INCp)Re(CO)$_3$] solutions has shown paramagnetic signals with hyperfine coupling on ^{14}N and ^{185}Re/^{187}Re nuclei (Fig. 1). EPR spectra modeling used spin Hamiltonian in form $\hat{H} = \boldsymbol{g}_{iso}\mu_B H \boldsymbol{S}_z + A^{N_1}_{iso}\boldsymbol{S}\mathbf{I}^{N_1} + A^{N_2}_{iso}\boldsymbol{S}\mathbf{I}^{N_2} + A^{Re}_{iso}\boldsymbol{S}\mathbf{I}^{Re}$ ($\boldsymbol{S} = 1/2$, $\mathbf{I}^{N_1} = \mathbf{I}^{N_2} = 1$, and $\mathbf{I}^{Re} = 5/2$). Simulation of EPR spectra gave $\boldsymbol{g}_{iso} = 2.009$ for both compounds and hyperfine coupling constants $A^{N_1}_{iso} = A^{N_2}_{iso} = 0.726$ mT, $A^{Re}_{iso} = 0.462$ mT for [(NNCp)Re(CO)$_3$], and $A^{N_1}_{iso} = 0.905$ mT, $A^{N_2}_{iso} = 0.445$ mT, $A^{Re}_{iso} = 0.373$ mT for [(INCp)Re(CO)$_3$]. Calculated parameters are in good agreement with typical $\boldsymbol{g}_{iso}$, A^{Re}_{iso} and $A^{N_i}_{iso}$ values of nitronyl/imino nitroxides[6,12] and reduced derivatives of rhenium(I) tricarbonyl diimine complexes *fac*-[(*a*-diimine$^{-\bullet}$)Re^{I}(CO)$_3$(L)].[20–23] The high natural isotropic hyperfine splitting constant of Re nuclei[24] makes it possible to clearly observe their coupling with the unpaired electron of nitroxide fragments. According to the results of molecular DFT calculations (ORCA 4.2 quantum chemistry package[25] with range-separated LC-BLYP functional and def2-TZVPP basis set), the spin density is found to be mainly localized on {O←N=C–N–$^{\bullet}$O}/{N=C–N–$^{\bullet}$O} fragments and has a very small value at the rhenium(I) center (Fig. S1†). It is noteworthy that the Mulliken spin density values for [(NNCp)Re(CO)$_3$] (−0.017) are higher than for [(INCp)Re(CO)$_3$] (−0.005), which is consistent with higher values of A^{Re}_{iso} for nitronyl nitroxide compared to that of imino nitroxide.

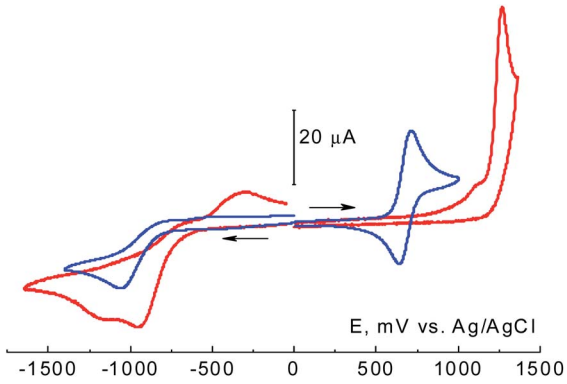

Fig. 2 CV curves of oxidation and reduction of [(NNCp)Re(CO)$_3$] (blue line), [(INCp)Re(CO)$_3$] (red line) 5.0×10^{-3} M solutions in MeCN (a GC disk electrode d = 1.7 mm, supporting electrolyte 0.1 M Bu_4NBF_4/MeCN, the scan rate 100 mV s^{-1}, T = 298 K).

According to the cyclic voltammetry (CV) data [(NNCp)Re(CO)$_3$] undergoes one-electron reversible oxidation (Fig. 2 and S2, ESI†). The value of the half-wave potential $E^{0\prime} = 681$ mV of the oxoammonium cation formation (Scheme 2) is comparable with the data for other reversibly oxidized nitronyl nitroxides.[12,26] The imino nitroxide [(INCp)Re(CO)$_3$] is oxidized irreversibly (Fig. 1); its oxidation potential is 557 mV higher than that of [(NNCp)Re(CO)$_3$], which could be associated with a much higher electron transfer energy and lower stability of the primary oxidation product (Scheme 2). At the higher anodic areas of 1400–2500 mV signals of subsequent irreversible oxidation processes for both [(NNCp)Re(CO)$_3$] and [(INCp)Re(CO)$_3$] were recorded (Fig. S3a and b, ESI†). [(NNCp)Re(CO)$_3$] and [(INCp)Re(CO)$_3$] are irreversibly reduced in the potential range of −950 to −1100 mV (Fig. 2), which is typical for most compounds containing a nitroxide fragment[12,27,28] due to the high basicity of the formed aminoxy anions (Scheme 2).[29] These results are in line with the data on the electrochemical behavior of the dihydroxyimidazolidine precursor – [(BHACp)Re(CO)$_3$] (Fig. S3c, ESI†), which can be considered as a product of complete reduction of [(NNCp)Re(CO)$_3$]. [(BHACp)Re(CO)$_3$] could not be reduced in the experimentally available potential

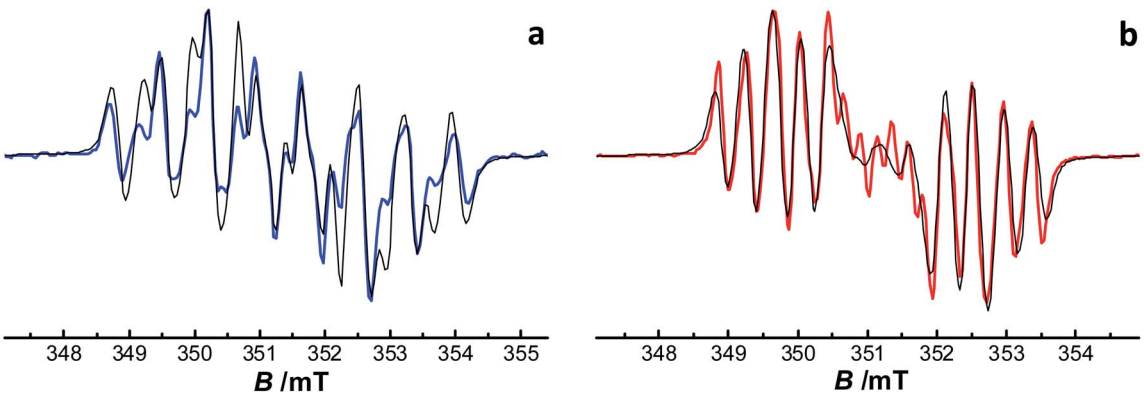

Fig. 1 Experimental EPR spectra for [(NNCp)Re(CO)$_3$] (a, blue curve) and [(INCp)Re(CO)$_3$] (b, red curve) recorded at room temperature in a degassed and diluted toluene solutions and their simulation (solid thin black curves).

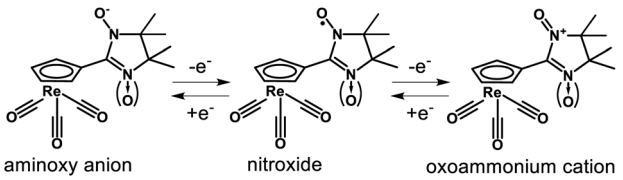

Scheme 2

range, but it is irreversibly oxidized at E^{p}_{ox} = 886 mV with a number of subsequent electrochemical transformations in higher anodic areas. Thus, external electrochemical impact on [(NNCp)Re(CO)$_3$] and [(INCp)Re(CO)$_3$] induces electron transfer only for the nitroxide fragment of the molecules, while their cyrhetrene moiety remains unchanged.

X-ray diffraction study of [(NNCp)Re(CO)$_3$], [(INCp)Re(CO)$_3$] (Fig. 3) and their diamagnetic precursor [(BHACp)Re(CO)$_3$] (Fig. S4, ESI†) showed that the bond lengths in coordination sphere of Re and >N–˙O groups are in good agreement with the previously reported ones for other cyrhetrenes and nitroxides species[30] (Re–C_{CO} – 1.86–1.92 Å, Re–C_{Cp} – 2.27–2.35 Å, N–O – 1.25–1.30 Å, Table S2, ESI†).

The formation of polymorphic modifications seems to be inherent in the nature of [(NNCp)Re(CO)$_3$]. We did obtain crystals of three polymorphs (here and further appointed as I, II and III). The crystal structures of II and III are formed by two crystallographically independent molecules – IIa, IIb and IIIa, IIIb, respectively (Fig. 3 and Table 1). The {ONCN(O)} nitroxide fragment and the Cp ring are practically coplanar for the most solids under study, which could be favorable for the spread of the spin density to the conjugated aromatic {ONCN(O)–Cp} system.[6,7]

Polymorphs of [(NNCp)Re(CO)$_3$] differ in the type and parameters of intermolecular contacts. Of particular interest is the environment of >N–˙O groups, since almost all of the spin density is concentrated on their π-antibonding orbitals (Fig. S1†). The efficiency of overlapping of these so-called magnetic orbitals,[31] is very important for the formation of channels of the strongest magnetic exchange interactions (Fig. 3, Tables 1 and 2).

Molecules a and b are combined into π-associated dimers with close location of >N–˙O groups in modifications II and III (II: $C_{Cp}\cdots C_{Cp}$ 3.38(2) Å and 3.4°, $N\cdots O_{NO}$ 3.69(1)/3.72(1) and $O_{NO}\cdots O_{NO}$ 3.82(1) Å; III: $C_{Cp}\cdots C_{Cp}$ 3.20(1) Å and 20.4°, $N\cdots O_{NO}$ 3.93(1)/3.94(1) and $O_{NO}\cdots O_{NO}$ and 4.07(1) Å; Fig. 3b and c). In addition, there are two pairs of short distances $O_{NO}\cdots C_{Cp}$ = 3.29(2) Å between IIb molecules. In polymorph III molecules IIIa are connected in a chain by a H-bond C_{Cp}–$H\cdots O_{NO}$ ($C\cdots O$ 3.20(3), $H\cdots O$ 2.33 Å). In the crystal structure of I, the distances both between neighboring >N–˙O groups and between the cyclopentadienyl ring and the nitroxide group are too large ($N\cdots O_{NO}$ and $O_{NO}\cdots O_{NO}$ > 4.5 Å, $O_{NO}\cdots C_{Cp}$ = 3.54(1) Å; Fig. 3a) to expect any significant magnetic exchange interactions for this polymorph. π-associated dimers in [(INCp)Re(CO)$_3$] are connected into a ribbon by short contacts between O of nitroxide groups and C of cyclopentadienyl ring ($C_{Cp}\cdots C_{Cp}$ 3.33(2) Å and

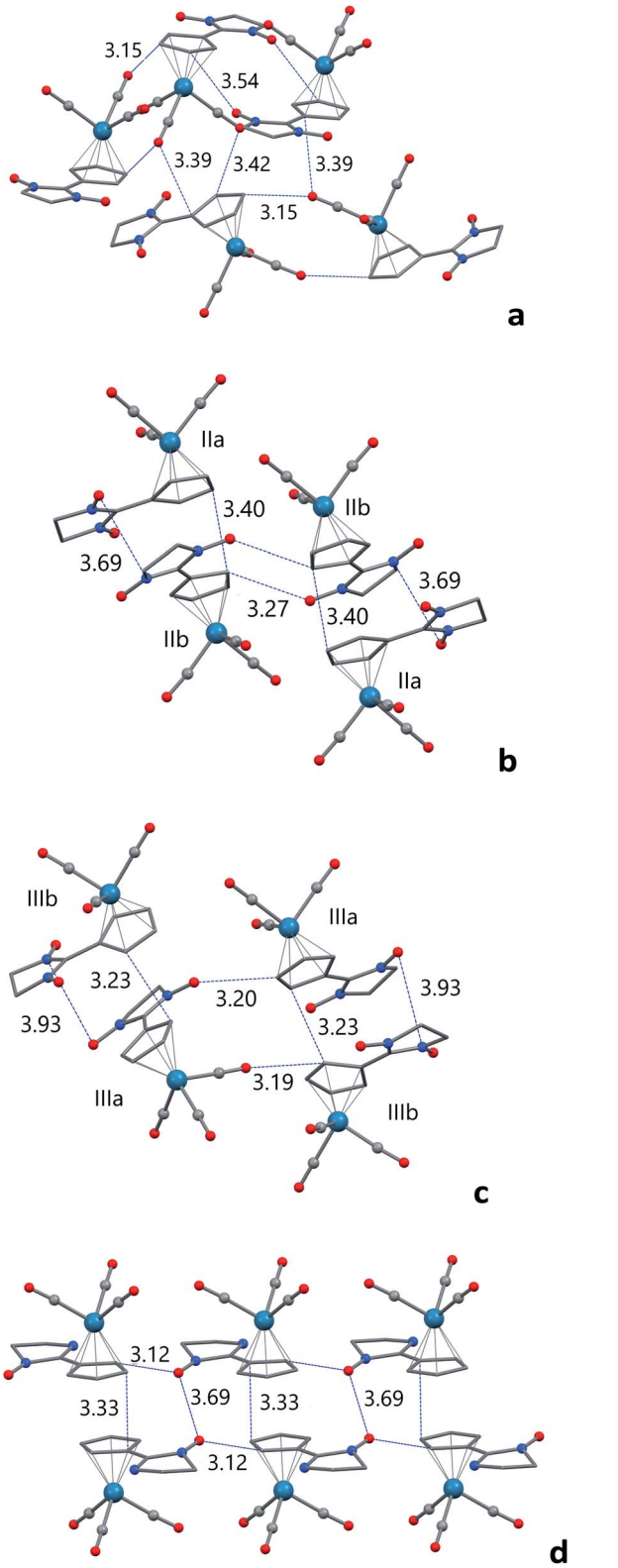

Fig. 3 Molecular structure and the shortest intermolecular distances (Å) of I (a), II (b), III (c) and [(INCp)Re(CO)$_3$] (d). The H atoms and the geminal CH_3 groups are omitted for clarity.

0°, $O_{NO}\cdots C_{Cp}$ = 3.12(1) Å; Fig. 3d). Distances $O_{NO}\cdots O_{NO}$ and $N\cdots O_{NO}$ between >N–˙O groups of adjacent π-dimers are 3.69(1) and 4.55(1) Å, respectively.

Table 1 Selected intermolecular distances (Å) and angles (°)

Compound		$O_{CO}\cdots O_{NO}$	$C_{Cp}\cdots C_{Cp}$ centroids	∠Cp⋯Cp	$Cp\cdots O_{NO}$	$O_{NO}\cdots O_{NO}$	$N\cdots O_{NO}$
$[(INCp)Re(CO)_3]$		3.95(1)	3.33(2)	0.0	3.12(1)–3.17(1)	**3.69(1)**	**4.55(1)**
$[(NNCp)Re(CO)_3]$	I	3.89(1)–3.81(1)	—	—	**3.54(1)**	—	—
	IIa–IIa	—	—	—	3.45(2)	4.16(1)	4.66(1)
	IIa–IIb	3.82(1)	3.38(2)	3.4	3.47(2)	**3.82(1)**	**3.69(1)–3.72(1)**
	IIb–IIb	3.98(1)–3.52(1)	—	—	3.29(2)–3.42(2)	4.44(2)	5.22(2)
	IIIa–IIIa	4.22(1)–4.06(1)	—	—	**3.20(3)**	—	—
	IIIa–IIIb	—	3.24(1)	20.4	3.60(1)	**4.07(1)**	**3.93(1)–3.94(1)**
	IIIb–IIIb	4.14(1)	—	—	—	—	—

The magnetochemical study confirmed that solids of the obtained nitroxides $[(NNCp)Re(CO)_3]$ and $[(INCp)Re(CO)_3]$ are paramagnetic (Fig. 4 and Table 2). For all studied spin-labeled derivatives of cyrhetrene the values of the effective magnetic moment μ_{eff} at 100–300 K are close to the theoretical spin-only value 1.73 μ_B for the monoradical with $\boldsymbol{S} = 1/2$ and $\boldsymbol{g} = 2$. There are no magnetic anomalies at the $\mu_{eff}(T)$ curves associated with intramolecular charge transfer or a change in the spin state of the nitroxide fragments and/or the Re^+ ion. Molecular DFT calculations (LC-BLYP/def2-TZVPP)[25] showed that the nearest in energy spin state isomers are above the ground state of the initial nitroxides by about 70 and 90 kcal M^{-1} for $[(NNCp)Re(CO)_3]$ and $[(INCp)Re(CO)_3]$, respectively. This manifests that the thermally induced spin state change-over or the intramolecular redox processes are energetically unfavorable.

A monotonic decrease of μ_{eff} with lowering temperature from 100 to 2 K indicates weak antiferromagnetic exchange interactions. Periodic DFT+*U* calculations[32] using the crystallographic geometry at room temperature of $[(NNCp)Re(CO)_3]$ and $[(INCp)Re(CO)_3]$ nitroxides revealed the most important passways of intermolecular magnetic exchange interactions (Table 2). In this respect, the most effective is the close mutual arrangement of >N–˙O groups in the π-associated dimers of polymorphs II and III. The calculated values of exchange interactions are $J^{calc}_{II\text{-}NO\cdots ON} = -15.6$ cm^{-1} and $J^{calc}_{III\text{-}NO\cdots ON} = -5.3$ cm^{-1}. These differences in the values of intermolecular magnetic exchange interactions are in good agreement with the best fit parameters within the same exchange-coupled dimer model: $J_{II} = -20.6$ cm^{-1} ($g_{II} = 1.93$) and $J_{III} = -12.3$ cm^{-1} ($g_{III} = 2.03$).

The magnitude of intermolecular exchange interactions, formed by the overlapping of the magnetic orbitals of the >N–˙O group and the Cp fragment of neighboring molecules, was estimated too. For modification I, where there are no other contacts between the spin density bearing fragments (Fig. 3a), the calculated value $J^{calc}_{I\text{-}NO\cdots Cp} = -1.4$ cm^{-1} agrees with the value of the exchange parameter $J_I = -2.0$ cm^{-1} ($g_I = 2.03$) obtained by fitting the experimental data. Among all the studied nitroxides, the shortest $O_{NO}\cdots C_{Cp}$ contacts were found for III; they bind IIIa molecules in the chain. The calculated $J^{calc}_{III\text{-}NO\cdots Cp}$ values are also very small (−1.8 cm^{-1}). Comparison of the calculated values of the exchange integrals $J^{calc}_{III\text{-}NO\cdots ON}$ and $J^{calc}_{III\text{-}NO\cdots Cp}$ for III confirms that the direct overlap of the magnetic orbitals of the >N–˙O groups of adjacent molecules is most effective for the onset of the strongest magnetic exchange interactions. The contribution of the exchange channels passing through the Cp fragments should be insignificant due to the poor transmitting of the spin density *via* the α-carbon atom to substituents of 2-imidazoline nitroxides.[6]

Periodic DFT calculations for $[(INCp)Re(CO)_3]$ revealed only weak antiferromagnetic exchange interactions $J^{calc}_{IN\text{-}NO\cdots ON} =$

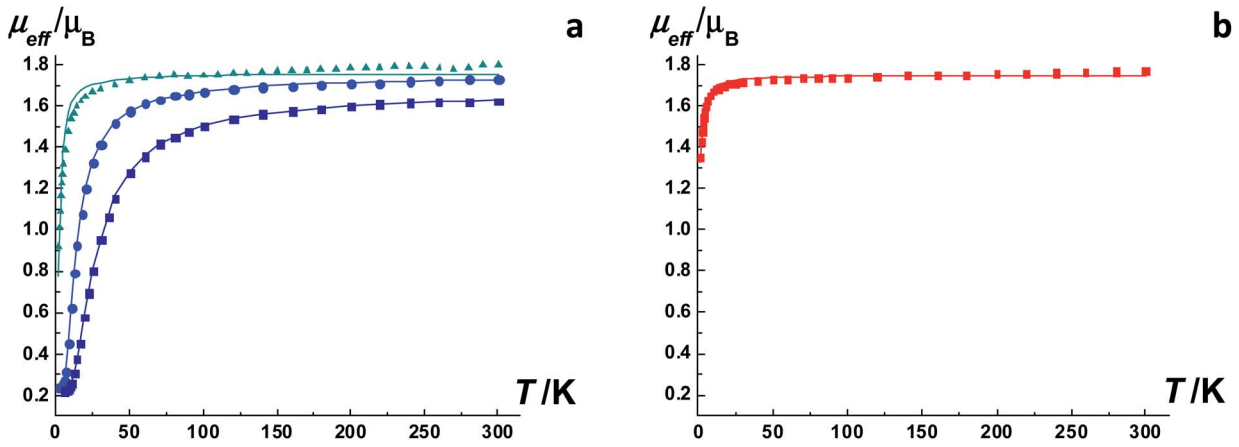

Fig. 4 Experimental dependences $\mu_{eff}(T)$ for the polymorphs of nitronyl nitroxide $[(NNCp)Re(CO)_3]$ (a: I – dark cyan triangles; II – dark blue squares; III – blue cycles) and imino nitroxide $[(INCp)Re(CO)_3]$ (b: red squares). Solid thick lines – fitted data based on optimized parameters (Table 2).

Table 2 The intermolecular exchange coupling parameters (cm^{-1}) according to results of analysis and fitting of magnetochemistry data (fitted) and periodical quantum-chemical calculations (calculated; Quantum Espresso 6.2 package,[32] PBE+*U*)

		Fitted			Calculated		
Compound		J	g	Spin Hamiltonian[33]	J	Contact type	Spin Hamiltonian[33]
[(INCp)Re(CO)$_3$]		−1.0	2.02	$H = -2JS_{R_1}S_{R_2}$, $S_{R_1} = S_{R_2} = \frac{1}{2}$	−2.6[a]	NO…ON	$H = -2JS_{R_1}S_{R_2}$, $S_{R_1} = S_{R_2} = \frac{1}{2}$
[(NNCp)Re(CO)$_3$]	I	−2.0	2.03		−1.4	Cp⋯ON	
	II	−20.6	1.93		−15.6	NO…ON	
					−5.3	NO…ON	
	III	−12.3	2.03		−1.8	Cp⋯ON	$H = -2J_{chain}\sum_{i=1}^{n-1} S_{R_i}S_{R_{i+1}}$, $S_{R_i} = \frac{1}{2}$

[a] The molecular DFT calculation[25] (LC-BLYP functional/def2-TZVPP) gave a similar evaluation $-J^{calc}_{IN\text{-}NO\cdots ON} = -0.75\ cm^{-1}$.

$-2.6\ cm^{-1}$ for dimers with the most closely located >N–˙O groups (Fig. 3d, Tables 1 and 2). These data are consistent with the values obtained by fitting the experimental dependence $\mu_{eff}(T)$ for exchange-coupled dimers: $J_{IN} = -1.0\ cm^{-1}$ and $g_{IN} = 2.02$ (Fig. 4b). This type of mutual arrangement of >N–˙O groups does not provide reliable overlap of their magnetic orbitals that determines the low efficiency of this channel of intermolecular magnetic exchange interactions.

Conclusions

Thus, the paramagnetic tricarbonyl half-sandwich rhenium(I) complexes [(NNCp)Re(CO)$_3$] and [(INCp)Re(CO)$_3$] with cyclopentadienyl-substituted nitronyl nitroxide NNCp and imino nitroxide INCp ligands were obtained as a result of this study. The correlation between the mutual arrangement of paramagnetic molecules in the solid phases of polymorphs [(NNCp)Re(CO)$_3$] and the energy of their magnetic exchange interactions was established. High kinetic stability of [(NNCp)Re(CO)$_3$] and [(INCp)Re(CO)$_3$] is of particular interest for the design of new multifunctional targeted drugs on their basis.

Author contributions

The manuscript was written through contributions of all authors. V. O. and K. M. developed the main conception and conceived the synthesis and physicochemical study of Re(I)-nitroxide complexes; V. O. and M. E. served as scientific advisors. K. M. synthesized of the Re(I)-nitroxide complexes under study. E. S., M. S. and M. E. performed the CV measurements and analysis; S. T., S. V. and M. F. studied Re(I)-nitroxide complexes by the EPR spectroscopy. G. R. and G. L. carried out X-ray experiment, refined the X-ray data and solved structures; A. B. performed the magnetochemistry measurements and analysis; V. M. carried out the quantum chemical calculations. All authors contributed in analysis and interpretation of obtained data and co-wrote the paper. K. M., G. R., and M. F. drafted the manuscript. All authors gave approvals to the final version of the manuscript.

Conflicts of interest

There are no conflicts to declare.

Acknowledgements

This work was supported by the Russian Foundation for Basic Research (Grant No. 19-29-08005, synthesis, electrochemical measurements and magnetochemistry studies) and the Russian Science Foundation (Grant No. 17-13-01022, XRD study).

References

1 E. B. Bauer, A. A. Haase, R. M. Reich, D. C. Crans and F. E. Kühn, *Coord. Chem. Rev.*, 2019, **393**, 79–117.
2 *Bioorganometallic Chemistry: Applications in Dug Discovery, Biocatalysis, and Imaging*, ed. G. Jaouen and M. Salmain, Wiley-VCH Verlag GmbH & Co, Weinheim, Germany, 2015, p. 398.
3 S. Hostachy, C. Policar and N. Delsuc, *Coord. Chem. Rev.*, 2017, **351**, 172–188.
4 A. Leonidova and G. Gasser, *ACS Chem. Biol.*, 2014, **9**, 2180–2193.
5 N. Lepareur, F. Lacoeuille, C. Bouvry, F. Hindré, E. Garcion, M. Chérel, N. Noiret, E. Garin and F. F. R. Knapp, *Front. Med.*, 2019, **6**, 00132.
6 *Stable Radicals: Fundamentals and Applied Aspects of Odd-Electron Compounds*, ed. R. G. Hicks, John Wiley & Sons, Ltd., 2010.
7 E. V. Tretyakov and V. I. Ovcharenko, *Russ. Chem. Rev.*, 2009, **78**, 971–1012.
8 V. I. Ovcharenko, E. Yu. Fursova, T. G. Tolstikova, K. N. Sorokina, A. Y. Letyagin and A. A. Savelov, *Dokl. Chem.*, 2005, **404**, 171–173.
9 N. A. Artyukhova, G. V. Romanenko, E. Y. Fursova and V. I. Ovcharenko, *RF Pat.*, RU2642468C2, 2015.
10 W. Owtscharenko, W. Huber and K. E. Schwarzhans, *Z. Naturforsch., B: J. Chem. Sci.*, 1986, **41**, 1587–1588.
11 Y. Nakamura, N. Koga and H. Iwamura, *Chem. Lett.*, 1991, **20**, 69–72.

12 O. Jürgens, J. Vidal-Gancedo, C. Rovira, K. Wurst, C. Sporer, B. Bildstein, H. Schottenberger, P. Jaitner and J. Veciana, *Inorg. Chem.*, 1998, **37**, 4547–4558.
13 C. Sporer, D. Ruiz-Molina, K. Wurst, H. Kopacka, J. Veciana and P. Jaitner, *J. Organomet. Chem.*, 2001, **637–639**, 507–513.
14 A. R. Forrester, S. P. Hepburn, R. S. Dunlop and H. H. Mills, *J. Chem. Soc. D*, 1969, 698–699.
15 S. Nakatsuji, K. Fujiwara, H. Akutsu, J. Yamada and M. Satoh, *New J. Chem.*, 2013, **37**, 2468–2472.
16 E. F. Ullman, J. H. Osiecki, D. G. B. Boocock and R. Darcy, *J. Am. Chem. Soc.*, 1972, **94**, 7049–7059.
17 J. Becher and E. F. Ullman, *US Pat.*, 3927019, 1975.
18 V. W.-W. Yam, K. K.-W. Lo and K. M.-C. Wong, *J. Organomet. Chem.*, 1999, **578**, 3–30.
19 A. Lannes, Y. Suffren, J. B. Tommasino, R. Chiriac, F. Toche, ¸L. Khrouz, F. Molton, C. Duboc, I. Kieffer, J.-L. Hazemann, C. Reber, A. Hauser and D. Luneau, *J. Am. Chem. Soc.*, 2016, **138**, 16493–16501.
20 T. Scheiring, A. Klein and W. Kaim, *J. Chem. Soc., Perkin Trans. 2*, 1997, 2569–2571.
21 A. Klein, C. Volger and W. Kaim, *Organometallics*, 1996, **15**, 236–244.
22 I. Löw, M. Bubrin, A. Paretzki, J. Fiedler, S. Záliš and W. Kaim, *Inorg. Chim. Acta*, 2017, **455**, 540–548.
23 P. A. Abramov, A. A. Dmitriev, K. V. Kholin, N. P. Gritsan, M. K. Kadirov, A. L. Gushchin and M. N. Sokolov, *Electrochim. Acta*, 2018, **270**, 526–534.
24 B. A. Goodman and J. B. Raynor, *Adv. Inorg. Chem. Radiochem.*, 1970, **13**, 135–362.
25 F. Neese, *Wiley Interdiscip. Rev.: Comput. Mol. Sci.*, 2012, **2**, 73–78.
26 Y. G. Budnikova, T. V. Gryaznova, M. K. Kadirov, E. V. Tret'yakov, K. V. Kholin, V. I. Ovcharenko, R. Z. Sagdeev and O. G. Sinyashin, *Russ. J. Phys. Chem. A*, 2009, **83**, 1976–1980.
27 A. S. Mendkovich, V. B. Luzhkov, M. A. Syroeshkin, V. D. Sen, D. I. Khartsii and A. I. Rusakov, *Russ. Chem. Bull.*, 2017, **66**, 683–689.
28 V. D. Sen', I. V. Tikhonov, L. I. Borodin, E. M. Pliss, V. A. Golubev, M. A. Syroeshkin and A. I. Rusakov, *J. Phys. Org. Chem.*, 2015, **28**, 17–24.
29 F. G. Bordwell and W.-Z. Liu, *J. Am. Chem. Soc.*, 1996, **118**, 8777–8781.
30 Cambridge Structural Database, *Ver. 5.42*, University of Cambridge, UK, 2020.
31 O. Kahn, *Molecular Magnetism*, Wiley-VCH, Weinheim, 1993.
32 P. Giannozzi, S. Baroni, N. Bonini, M. Calandra, R. Car, C. Cavazzoni, D. Ceresoli, G. L. Chiarotti, M. Cococcioni, I. Dabo, A. Dal Corso, S. de Gironcoli, S. Fabris, G. Fratesi, R. Gebauer, U. Gerstmann, C. Gougoussis, A. Kokalj, M. Lazzeri, L. Martin-Samos, N. Marzari, F. Mauri, R. Mazzarello, S. Paolini, A. Pasquarello, L. Paulatto, C. Sbraccia, S. Scandolo, G. Sclauzero, A. P. Seitsonen, A. Smogunov, P. Umari and R. M. Wentzcovitch, *J. Phys.: Condens. Matter*, 2009, **21**, 395502.
33 R. Boča, *A Handbook of Magnetochemical Formulae*, Elsevier Inc., 2012, p. 1010.